Inorg. Chem. **2002**, *41*, 1698–1700

Observation of the Structural Consequences of a Reversible $S = {}^3/_2$ and $S = {}^1/_2$ Spin Crossover in the Single Crystal

Yoshiki Ohgo,*,† Takahisa Ikeue,† and Mikio Nakamura*,†,‡

Department of Chemistry, Toho University School of Medicine, Ota-ku, Tokyo 143-8540, Japan, and Division of Biomolecular Science, Graduate School of Science, Toho University, Funabashi, Chiba 274-8510 Japan

Received December 3, 2001

Highly saddle shaped iron(III) porphyrin complex **1** showing a novel spin crossover process between the $S = {}^3/_2$ and $S = {}^1/_2$ has been crystallographically analyzed at 298, 180, and 80 K. As the temperature is lowered, the lattice contraction has occurred specifically along the *b*-axis. Correspondingly, the iron–pyridine bonds, which tilt slightly from the *b*-axis, have decreased by 7.3%. In contrast, the lattice contractions along the *a*- and *c*-axes are much smaller and the iron–porphyrin bonds, which almost coincide with the *a*- and *c*-axes, have shown much smaller contraction, ca. 2.2%. The large contraction of the specific bonds caused by packing force raises the energy level of the d_{z^2} orbital and induces the spin transition. The detailed structural and lattice changes in the single crystal, which may be regarded as a superstructure parallel to a protein matrix, have been clarified.

One of the challenging projects in chemistry and biochemistry is to monitor the reaction process directly by X-ray analysis.[1] We have recently reported that the six-coordinated iron(III) complexes with saddle-shaped porphyrin such as $[Fe(OETPP)Py_2]ClO_4$ and $[Fe(OETPP)(4\text{-}CNPy)_2]ClO_4$ show a novel spin crossover process from the $S = {}^3/_2$ to the $S = {}^1/_2$ as the temperature is lowered.[2,3] Thus, these complexes are quite suitable to monitor crystallographically how the coordination structure and the surrounding lattice change during the spin transition process. Here, we report the X-ray crystallographic analysis of $[Fe(OETPP)Py_2]ClO_4$ (**1**) at three different temperatures and explain why the novel spin transition takes place in this complex from the viewpoint of crystal structure.

1 was synthesized according to the literature methods.[2,4] The solid obtained was recrystallized from CH_2Cl_2 solution. A purple prismatic crystal of **1** having approximate dimensions of 0.2 × 0.2 × 0.1 mm was mounted on a glass fiber. All data sets were collected on a Rigaku RAXIS-RAPID imaging plate diffractometer with Mo Kα radiation (λ = 0.71069 Å). Indexing was performed from 2 oscillations which were exposed for 1.7 min. The camera radius was 127.40 mm. Readout was performed in the 0.100 mm pixel mode. The data were collected to a maximum 2θ value of 55°. A total of 110 images, corresponding to 386.5° oscillation angles, were collected with 3 different goniometer settings. Exposure time was 2.00 min/deg. Data were processed by the PROCESS-AUTO program package. A symmetry-related absorption correction was made using the program ABSCOR. The structures were solved by direct methods with the program SIR97 in TEXSAN and expanded using the program DIRDIF94.[5] The structure refinement was carried out by full-matrix least-squares refinement with SHELXL-97 against F^2.[5] All non-hydrogen atoms were refined anisotropically. All the hydrogen atoms were generated geometrically. The positional parameters of the H atoms were constrained to have C−H distances of 0.96 Å for primary, 0.97 Å for secondary, and 0.93 Å for aromatic H atoms. The H-atom *U* values were constrained to have 1.2 times the equivalent isotropic *U* value of their attached atoms

* To whom correspondence should be addressed. E-mail: yohgo@med.toho-u.ac.jp (Y.O.); mnakamu@med.toho-u.ac.jp (M.N.).

† Toho University School of Medicine.

‡ Division of Biomolecular Science, Graduate School of Science, Toho University.

(1) Scheidt, W. R.; Geiger, D. K.; Haller, K. J. *J. Am. Chem. Soc.* **1982**, *104*, 495−499.

(2) Ikeue, T.; Ohgo, Y.; Yamaguchi, T.; Takahashi, M.; Takeda, M.; Nakamura, M. *Angew. Chem., Int. Ed.* **2001**, *40*, 2617−2620.

(3) Abbreviations: OETPP, dianion of 2,3,7,8,12,13,17,18-octaethyl-5,10,15,20-tetraphenylporphyrin; Py, pyridine; 4-CNPy, 4-cyanopyridine; DMAP, *N*,*N*-(dimethylamino)pyridine.

(4) Barkigia, K. M.; Berber, M. D.; Fajer, J.; Medforth, C. J.; Renner, M. W.; Smith, K. M. *J. Am. Chem. Soc.* **1990**, *112*, 8851−8857.

(5) (a) TEXSAN: Crystal Structure Analysis Package, Molecular Structure Corporation (1985 & 1999). TEXSAN. TEXRAY Structure Analysis Package. MSC, 3200 Research Forest Drive, The Woodlands, TX 77381. (b) SV: Nemoto, T.; Ohashi, Y. 1993. SV. Program for Crystal and Molecular Graphics. Tokyo Institute of Technology, Japan. (c) ABSCOR: Higashi, T. 1995. Program for Absorption Correction, Rigaku Corporation, Tokyo, Japan. (d) SIR97: Altomare A.; Burla, M. C.; Camalli, M.; Cascarano, G. L.; Giacovazzo, C.; Guagliardi, A.; Moliterni, A. G. G.; Polidori, G.; Spagna, R. *J. Appl. Crystallogr.* **1999**, *32*, 115. (e) ORTEP: Johnson, C. K. 1965. ORTEP. Report ORNL-3794. Oak Ridge National Laboratory, Oak Ridge, TN. (f) SHELXL-97: Sheldrick, G. M. 1997. SHELXL97. Program for the Refinement of Crystal Structures. University of Göttingen, Germany. (g) DIRDIF94: Beurskens, P. T.; Admiraal, G.; Beurskens, G.; Bosman, W. P.; Gelder, R. de; Israel, R.; Smits, J. M. M. 1994. The DIRDIF-94 program system, Technical Report of Crystallography Laboratory, University of Nijmengen, The Netherlands.

10.1021/ic015620v CCC: $22.00
Published on Web 03/14/2002

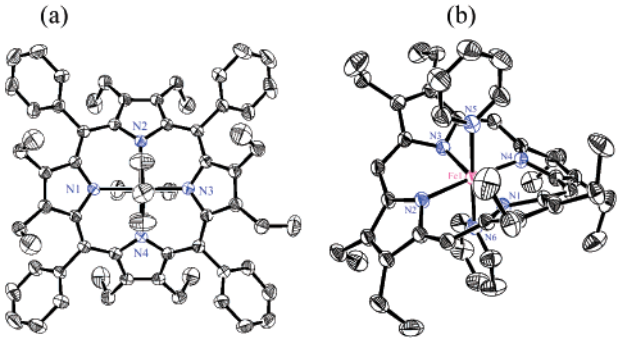

Figure 1. ORTEP diagram of **1** with the atomic numbering. Displacement ellipsoids are shown at the 30% probability level. (a) Top view. (b) Side view. Phenyl rings are omitted for clarity.

Table 1. Crystallographic Details for $[Fe(OETPP)Py_2]ClO_4$ at Three Different Temperatures

	298 K	180 K	80 K
formula		$C_{70}H_{70}N_6FeClO_4 \cdot 2CH_2Cl_2$	
mol wt		1320.47	
cryst syst		monoclinic	
space group		$P2_1/n$	
Z		4	
a (Å)	13.972(1)	13.800(2)	13.857(1)
b (Å)	19.481(1)	17.870(2)	17.764(1)
c (Å)	26.750(3)	26.237(3)	26.184(2)
β (deg)	101.493(3)	101.375(3)	101.411(1)
V (Å^3)	6969.0(10)	6343.3(12)	6318.0(6)
R1	0.0759	0.0943	0.0923
wR2	0.2435	0.1958	0.2016
GOF	1.073	0.978	1.010

(1.5 for methyl groups). The atomic scattering factors were taken from *International Tables for Crystallography*.

Result and Discussion

The X-ray structure analysis has been carried out at 80, 180, and 298 K. The crystal data of **1** are listed in Table 1. The space group is maintained throughout the temperature range examined. As the temperature is lowered from 298 to 80 K, the volume of the unit cell has decreased by 6.7%. Figure 1 shows the molecular structure of **1** together with numbering, which clearly exhibits the highly saddled structure.[4,6−8] The maximum deviation within the $C_{20}N_4Fe$ core, 1.312(3) Å, is observed for one of the β-pyrrole carbon atoms as shown in Figure 2. Deviation of *meso* carbons from the least-squares plane of the $C_{20}N_4Fe$ core is fairly small, 0.05 Å, showing the considerably pure saddled conformation, in contrast to that of the analogous $[Fe(OETPP)(DMAP)_2]^+$, 0.31 Å, reported recently.[8] This is probably because of the orientation of DMAP ligand due to the short $Fe-N_{ax}$ bond length of $[Fe(OETPP)(DMAP)_2]^+$. Table 2 lists the axial and equatorial bond lengths at three different temperatures. These data indicate that most of the bonds contract at lower

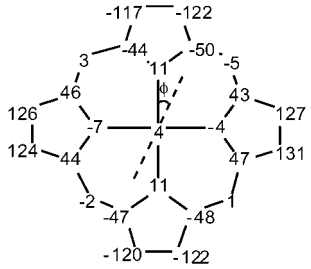

Figure 2. Formal diagram of porphyrin core of **1** showing displacements of each atom from the least-squares plane of the $C_{20}N_4$ porphyrinato core at 298 K in units of 0.01 Å. The dihedral angle between the coordinated pyridine and N_p-Fe-N_{axial}, ϕ, is 3.6° at this temperature.

Table 2. Fe−N Bond Lengths of $[Fe(OETPP)Py_2]ClO_4$

	bond lengths (Å)		
bonds	298 K	180 K	80 K
Fe1−N1	1.967(2)	1.950(3)	1.960(3)
Fe1−N2	1.997(3)	1.958(3)	1.955(3)
Fe1−N3	1.975(2)	1.953(3)	1.965(3)
Fe1−N4	2.000(3)	1.954(3)	1.947(3)
Fe1−N5	2.197(3)	2.039(4)	2.001(3)
Fe1−N6	2.204(3)	2.042(4)	1.984(3)
$Fe-N_p$[a]	1.985(3)	1.954(3)	1.957(3)
$Fe-N_{ax}$[b]	2.201(3)	2.041(4)	1.993(3)

[a] Average bond length of the equatorial bonds. [b] Average bond length of the axial bonds.

temperature. The shortening of the axial bonds is much larger than that of the equatorial ones. The average axial and equatorial bonds, $Fe-N_{ax}$ and $Fe-N_p$, have shown 9.5% and 1.4% contraction, respectively, as the temperature is lowered from 298 to 80 K. The data in Table 2 also demonstrate that the bond contraction between 298 and 180 K is much larger than that between 180 and 80 K; the bond contraction for $Fe-N_{ax}$ is 0.160 and 0.048 Å for each temperature range, respectively, while that for $Fe-N_p$ is 0.031 and <0.01 Å.

Another notable change in structure has been observed in the rotation angle ϕ of the pyridine ligand; ϕ is defined as the dihedral angle between the coordinated pyridine and N_p-Fe-N_{ax} planes as shown in Figure 2. The pyridine ligands are placed almost along the diagonal N_p-Fe-N_p axes perpendicularly above and below the porphyrin; ϕ is fairly small, 3.6°, at 298 K. The rotation angle has increased, however, from 3.6° to 6.0° (180 K), and then to 9.7° (80 K). The increase in the rotation angle should be ascribed to the shortening of the $Fe-N_{ax}$ bond at lower temperature. Because of the bond contraction, the steric repulsion between the ligand and pyrrole nitrogen atoms would increase. Thus, the conformation at $\phi = 3.6°$, which is most stable at 298 K where $Fe-N_{ax}$ is 2.201 Å, is no longer stable at 80 K where $Fe-N_{ax}$ is 1.993 Å. To minimize the steric repulsion increase at lower temperature, the planar ligand must rotate. It should be noted that, in contrast to the case of $Fe-N_{ax}$ bond length, the rotation angle has increased to a greater extent as the temperature is lowered from 180 to 80 K than from 298 to 180 K. The result suggests that the steric repulsion between the ligand and the pyrrole nitrogen increases to a greater extent when the $Fe-N_{ax}$ bond shortens from 2.041 Å (180 K) to 1.993 Å (80 K) than it decreases from 2.201 Å (298 K) to 2.041 Å (180 K).

(6) Shelnutt, J. A.; Song, X.-Z.; Ma, J.-G.; Jia, S.-L.; Jentzen, W.; Medforth, C. J. *Chem. Soc. Rev.* **1998**, *27*, 31−41.
(7) (a) Cheng, R.-J.; Chen, P.-Y.; Gau, P.-R.; Chen, C.-C.; Peng, S.-M. *J. Am. Chem. Soc.* **1997**, *119*, 2563−2569. (b) Schünemann, V.; Gerdan, M.; Trautwein, A. X.; Haoudi, N.; Mandon, D.; Fischer, J.; Weiss, R.; Tabard, A.; Guilard, R. *Angew. Chem., Int. Ed.* **1999**, *38*, 3181−3183.
(8) Ogura, H.; Yatsunyk, L.; Medforth, C. J.; Smith, K. M.; Barkigia, K. M.; Renner, M. W.; Melamed, D.; Walker, F. A. *J. Am. Chem. Soc.* **2001**, *123*, 6564−6578.

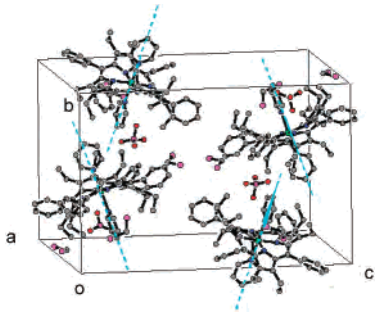

Figure 3. The crystal structure of **1** obtained at 298 K. The light blue lines show the N5−Fe−N6 axes.

We then examined if the structural data of **1** correlate with the magnetic and spectroscopic data reported in our previous paper.[2] The temperature dependence of the effective magnetic moment (μ_{eff}) determined for a microcrystalline sample by SQUID magnetometry qualitatively correlates with the structural data. The μ_{eff} value decreased from 3.43 to 2.69μ_B as the temperature was lowered from 298 to 180 K, while it decreased to a smaller extent, from 2.69 to 2.43 μ_B, as the temperature was further lowered from 180 to 80 K.[9] A similar tendency was observed in the Mössbauer parameters; the quadrupole splitting and isomer shift decreased by 0.43 and 0.07 mm s^{-1}, respectively, on going from 298 to 180 K, while they exhibited a much smaller decrease, 0.04 and 0.00 mm s^{-1}, on going from 180 to 80 K. These results clearly indicate that the contraction of the axial bonds is closely related to the spin transition from $S = {}^3/_2$ to $S = {}^1/_2$.

Let us now consider why the novel spin crossover process takes place in the crystal. Figure 3 shows the crystal structure of **1** obtained at 298 K. As the temperature is lowered, the thermal motion of the molecules, especially that of the peripheral substituents, is restrained. The low temperature also decreases the thermal motion of each bond, inducing the bond contraction. As a result, the void space around the molecules increases, which requires the realignment of each molecule to achieve better crystallinity for the contracted molecules. In fact, the unit cell has decreased by 6.3% in volume on going from 298 to 180 K, as if it suffers from the external force, i.e., packing force. It should be noted that the *a*- and *c*-axes almost coincide with the N1−N3 and N2−N4 axes, respectively. The *b*-axis tilts from the N5−N6 axis by ca. 15°. Close examination of the crystal data in Table 1 reveals that the lattice contraction along the *a*-, *c*-, and *b*-axes are 1.2%, 1.9%, and 3.3%, respectively, in the temperature range 298−180 K. Correspondingly, the bond contraction takes place by 1.0%, 2.2%, and 7.3% for Fe1−N1(N3), Fe1−N2(N4), and Fe1−N5(N6), respectively. It should be noted that, as the temperature is lowered from 298 to 180 K, the largest contraction of the unit cell occurs along the *b*-axis, which results in the largest contraction of the Fe−N_{ax} bonds. This shortening of the axial bonds destabilizes the d_{z^2} orbital and induces the spin transition from $S = {}^3/_2$ to the $S = {}^1/_2$. The phenomenon observed in the crystal is closely connected with the functional tuning process of some heme proteins where the various vectorial interactions such as hydrogen bonding, dipolar interaction, steric repulsion, etc. are imposed on the active center. One of these examples is the structural change of leghemoglobin in the dioxygen binding process.[10] Orientation change of the proximal and distal histidine ligands together with the Fe−N bond contraction induces the change in the spin state. In this sense, the crystal of **1** may be regarded as a superstructure parallel to a protein matrix in its constraining function (see Supporting Information). In summary, we have shown a detailed structural and lattice change in the single crystal of **1** during the novel spin transition process.

Acknowledgment. We thank Professors Yuji Ohashi and Hidehiro Uekusa, Department of Chemistry, Faculty of Science, Tokyo Institute of Technology, for the assistance during the X-ray measurements. This work was supported by a Grant in Aid for Scientific Research on Priority Areas (A) (No. 12020257 to M.N.) from Ministry of Education, Culture, Sports, Science and Technology, Japan.

Supporting Information Available: Crystallographic information files (CIFs) and expanded discussions. This material is available free of charge via the Internet at http://pubs.acs.org.

IC015620V

(9) The mole fractions of the $S = {}^3/_2$ state are determined to be 0.73, 0.35, and 0.24 at 298, 180, and 80 K, respectively, on the basis of the effective magnetic moments.

(10) Harutyunyan, E. H.; Safonova, T. N.; Kuranova, I. P.; Popov, A. N.; Teplyakov, A. V.; Obmolova, G. V.; Rusakov, A. A.; Vainshtein, B. K.; Dodson, G. G.; Wilson, J. C.; Perutz, M. F. *J. Mol. Biol.* **1995**, *251*, 104−115.